Evidence for two distinct binding sites for tau on microtubules

Victoria Makrides[†], Michelle R. Massie[†], Stuart C. Feinstein[†], and John Lew[†‡§]

[†]Neuroscience Research Institute, Department of Molecular, Cellular, and Developmental Biology, and [‡]Biomolecular Sciences and Engineering Program, University of California, Santa Barbara, CA 93106

Communicated by John A. Carbon, University of California, Santa Barbara, CA, February 12, 2004 (received for review August 8, 2003)

The microtubule-associated protein tau regulates diverse and essential microtubule functions, from the nucleation and promotion of microtubule polymerization to the regulation of microtubule polarity and dynamics, as well as the spacing and bundling of axonal microtubules. Thermodynamic studies show that tau interacts with microtubules in the low- to mid-nanomolar range, implying moderate binding affinity. At the same time, it is well established that microtubule-bound tau does not undergo exchange with the bulk medium readily, suggesting that the tau–microtubule interaction is essentially irreversible. Given this dilemma, we investigated the mechanism of interaction between tau and microtubules in kinetic detail. Stopped-flow kinetic analysis reveals moderate binding affinity between tau and preassembled microtubules and rapid dissociation/association kinetics. In contrast, when microtubules are generated by copolymerization of tubulin and tau, a distinct population of microtubule-bound tau is observed, the binding of which seems irreversible. We propose that reversible binding occurs between tau and the surface of preassembled microtubules, whereas irreversible binding results when tau is coassembled with tubulin into a tau–microtubule copolymer. Because the latter is expected to be physiologically relevant, its characterization is of central importance.

The microtubule-associated protein (MAP) tau is a critical regulator of microtubule dynamics, and defects in microtubule dynamics have been shown to result in cell death (1). Furthermore, a number of mutations in the tau gene that are associated with frontotemporal dementia with parkinsonism linked to chromosome 17 have proven that tau dysfunction can play a causal role in the death of neurons (2). A characteristic defect associated with these mutations is a weaker interaction between tau and microtubules. Thus, knowledge of the detailed mechanism by which tau binds to microtubules is of crucial importance.

To date, no information is available on the kinetic steps involved in the binding process; rather, all studies on the mechanism of tau binding to microtubules have been thermodynamic in nature. Studies by Weingarten *et al*. (3) demonstrated that tau does not interconvert between differently radioactively tagged tubulin fractions through multiple cycles of polymerization and depolymerization. Thus, binding is inferred to be tight, perhaps irreversible. On the other hand, purified tau binds to microtubules with moderate as opposed to high affinity (4–10), and consequently the microtubule-bound and free forms of tau are expected to be readily exchangeable. Thus, not only is kinetic information lacking, but the available thermodynamic data also seem to be conflicting.

To address these issues, we carried out rapid-mixing stopped-flow kinetic experiments as well as equilibrium-competition binding studies to investigate the mechanism of interaction between tau and microtubules. Our data suggest that tau can bind to two distinct sites on microtubules: one that displays reversible binding kinetics with preassembled microtubules and a second in which tau becomes irreversibly bound if incorporated into microtubules during the microtubule polymerization process.

Experimental Procedures

Tau Purification and Acrylodan Labeling. Recombinant full-length adult human 4-repeat, 2N tau (441 aa) was overexpressed in *Escherichia coli* by using the pET vector expression system (Novagen) and HPLC-purified as described (11). The routine determination of tau protein concentration involved SDS/PAGE, Coomassie blue staining, and scanning densitometry using a tau protein standard, the concentration of which was calibrated by amino acid composition analysis. Purified tau was labeled to maximum stoichiometry with acrylodan (Molecular Probes), which modifies Cys-291 and Cys-322. Briefly, purified tau was reduced with a 10-fold molar excess of DTT for 2 h, desalted on a 5-ml column of Sephadex G-25, and then incubated with a 10-fold molar excess of acrylodan (2 h in the dark at room temperature) in BRB-80 buffer (80 mM Pipes/1 mM EGTA/1 mM $MgSO_4$, pH 6.8) in a final concentration of 10% DMSO. Unincorporated acrylodan was removed by chromatography on a Sephadex G-25 column equilibrated with BRB-80 buffer. Acrylodan-labeled tau (tau*) was resolved by SDS/PAGE and visualized by in-gel UV excitation before Coomassie staining. The stoichiometry of labeling was measured by fluorescence spectroscopy (excitation at 390 nm, emission at 490 nm) in 50% DMSO/BRB-80 using known concentrations of 2-mercaptoethanol-modified acrylodan as standard.

Preassembled Microtubules. Microtubule seeds were made by polymerizing tubulin in the presence of 10% glycerol and 10% DMSO followed by shearing of microtubules by passage through a 22-gauge syringe needle. Seeds then were used to nucleate the assembly of microtubules from MAP-free phosphocellulose-purified bovine tubulin (50 μM) at 32°C in BRB-80 buffer/1 mM GTP for $\geq$30 min, followed by the stepwise addition of increasing concentrations of taxol (Sigma) (diluted in DMSO) to a final concentration of 20 μM taxol/1% DMSO. Taxol-free microtubules were generated in the same way except that taxol was omitted. DMSO in these samples was 0.2% final. Taxol in this range did not affect interaction of microtubules with tau (data not shown).

Equilibrium Binding and Competition. Steady-state fluorescence emission was measured in a SPEX Fluorolog 3 spectrofluorometer (λ_{ex} = 280 nm, λ_{em} = 400–540 nm) at 25°C in BRB-80 buffer with GTP and/or taxol as indicated (see figure legends). In equilibrium binding experiments (see Fig. 3), aliquots of tau* were sequentially added to a fixed concentration of taxol-stabilized microtubules (change in volume was minimal), and the fluorescence emission at 497 nm was recorded. The signal caused by fluorescence resonance energy transfer (FRET) was taken as the difference in fluorescence intensity emitted from tau* in the presence versus the absence of microtubules. Eq. **1**,

Abbreviations: tau*, acrylodan-labeled tau; MAP, microtubule-associated protein; FRET, fluorescence resonance energy transfer.

[§]To whom correspondence should be addressed. E-mail: lew@lifesci.ucsb.edu.

www.pnas.org/cgi/doi/10.1073/pnas.0400992101

$$F = F_{max}(b - (b^2 - 4ac)^{0.5})/2a + y, \quad [1]$$

was fit to the data, where $b = a + c + K_D$, F is the fluorescence emission caused by FRET at any tau concentration, F_{max} is the fluorescence at saturating tau, a is the concentration of tau-binding sites, c is the concentration of tau*, and y is the y-intercept value.

In competition experiments (see Fig. 4), microtubules (50 μM tubulin) with or without taxol were incubated with tau* in the absence or presence of 10-fold molar excess unlabeled tau and simultaneously diluted 5-fold. Fluorescence emission caused by FRET was measured on samples after an additional 8-fold dilution in BRB-80 buffer with or without taxol. Alternatively, tubulin (10 μM) was copolymerized with tau* (2 μM) in the absence or presence of 10-fold molar excess unlabeled tau, and fluorescence measurements were taken after 8-fold dilution. In all experiments containing only tau*, unlabeled tau (10-fold excess over tau*) was then subsequently added as chase (change in volume was minimal).

Transient-State Kinetic Analysis. Stopped-flow kinetic experiments were conducted in an Applied Photophysics SX.18MV stopped-flow instrument (Applied Photophysics, Leatherhead, U.K.) fit with a 467-nm cut-off filter between the cuvette and photomultiplier tube (λ_{ex} = 280 nm, bandpass = 4 nm). Microtubules and tau* were mixed rapidly from syringes delivering equal-volume injections. All other buffer components, including GTP and taxol, were held constant in both syringes. All experiments were performed in BRB-80 buffer at 25°C.

Kinetic Data Analysis. A system of differential equations (available on request) describing schemes 1–3 (shown in Fig. 2), respectively, were globally fit to a family of kinetic traces corresponding to multiple concentrations of tau* at a single fixed concentration of taxol-stabilized microtubules. All traces are the average of three to five individual traces. Background fluorescence caused by direct excitation of acrylodan was subtracted from each of the averaged traces. An artifactual lag phase apparent in the first 1.5 ms at all tau* concentrations was omitted from each data set before fitting. Fitting was carried out by nonlinear least-squares regression analysis using numerical integration methods. Regression analysis and kinetic simulations were performed by using the software program SCIENTIST (MicroMath, Salt Lake City).

Results

Tau*. We developed a probe based on FRET that allowed robust measurement of the interaction of tau and microtubules. Tau contains two cysteine residues (Cys-291 and Cys-322) that can be labeled to stoichiometry by the fluorophore acrylodan, which serves as an efficient acceptor of energy transfer from donor tryptophans. Full-length human tau (tau 441) was labeled to stoichiometry, and the microtubule assembly activity of the tau* was tested in a conventional microtubule assembly assay. Acrylodan labeling showed modest effects on the ability of tau to assemble microtubules in terms of the extent of assembly and on the assembly half-time ($t_{1/2}$ = ≈15 min for unlabeled tau versus ≈25 min for tau*) (Fig. 1). However, the acrylodan-labeled material exhibited high assembly activity and strongly promoted tubulin polymerization, compared with a control that did not contain tau.

Excitation of microtubule-bound tau* at 280 nm resulted in an ≈6-fold increase in the relative fluorescence emission intensity at wavelength 500 nm in comparison with that of free tau* (data not shown). The fluorescence emission signal specifically caused by energy transfer was used as a reporter of tau binding to microtubules in all kinetic and equilibrium binding studies.

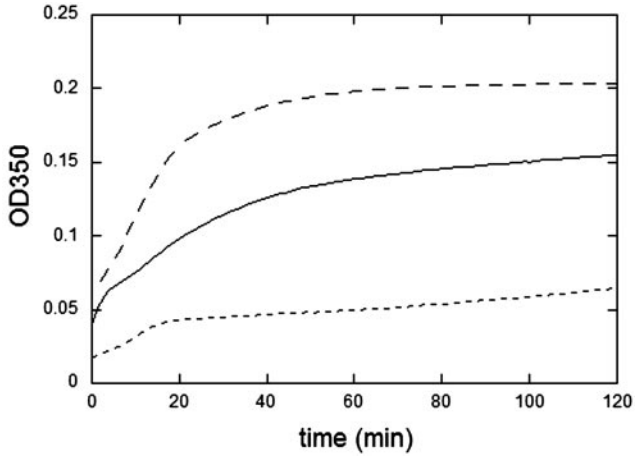

Fig. 1. Microtubule assembly competence of tau*. Tubulin (15 μM) was incubated with tau* (1.5 μM, —), unmodified tau (1.5 μM, – –), or no tau (- - -) at 35°C, and microtubule assembly was monitored by absorbance at A_{350} caused by light scattering. The reaction buffer was 50 mM Pipes, pH 6.8/1 mM EGTA/1 mM Mg_2SO_4/1 mM GTP.

Kinetic Pathway for the Binding of Tau to Microtubules. We analyzed the time course for tau* binding to microtubules, which was found to occur on the millisecond time scale monitored by rapid-mixing stopped-flow fluorescence spectroscopy. In this technique, taxol-stabilized microtubules were mixed rapidly with varying concentrations of tau*, and binding was monitored by the time-dependent increase in total fluorescence emission >467 nm as a result of energy transfer. Three hypothetical reaction schemes were considered as possible models for the observed binding kinetics (Fig. 2). The simplest scheme corresponds to a single-step reversible interaction between tau and microtubules to form the tau–microtubule complex (Fig. 2*A*, scheme 1). We also considered conformational changes in either the tau molecule or microtubules that may occur after (Fig. 2*B*, scheme 2) or before (Fig. 2*C*, scheme 3) bimolecular encounter.

The best-fit curves corresponding to each scheme are shown in Fig. 2. The data show that the binding of tau to microtubules under these conditions cannot be fit by a simple one-step binding mechanism (Fig. 2*A*). Rather, a mechanism involving a minimum of two steps is required, suggesting a conformational change (k_3, k_4) that occurs either before (Fig. 2*C*, scheme 3) or after (Fig. 2*B*, scheme 2) bimolecular encounter (k_1, k_2). Of the two possible schemes, scheme 3 provided a significantly better fit to the data (Fig. 2) both visually and by analysis of the residuals (data not shown). The optimized parameter values derived from this model are shown in Table 1. The kinetic constants correspond to an overall K_D value of 16 nM [$K_D = (k_2/k_1)(1 + k_4/k_3)$], whereas the optimized stoichiometry of binding was determined to be ≈1:3 (0.7/2.3) tau-binding sites per tubulin dimer. The K_D value and binding stoichiometry are consistent with corresponding values in the literature that have been reported by several laboratories (4–10).

Equilibrium Binding of Tau to Microtubules. We carried out equilibrium binding experiments to directly determine the overall K_D value. A plot of the equilibrium fluorescence intensity caused by energy transfer as a function of tau* concentration is shown in Fig. 3. A fit to these data using Eq. **1** provided values for both K_D and the maximal stoichiometry of binding (N). These values (K_D = 14 nM, N = 0.30) agree well with the stopped-flow kinetic data (K_D = 16 nM). Importantly, the K_D value of 14 nM is significantly different from that predicted when scheme 2 was assumed as the kinetic model [$K_D = (k_2/k_1)/(1 + k_3/k_4)$ = 142

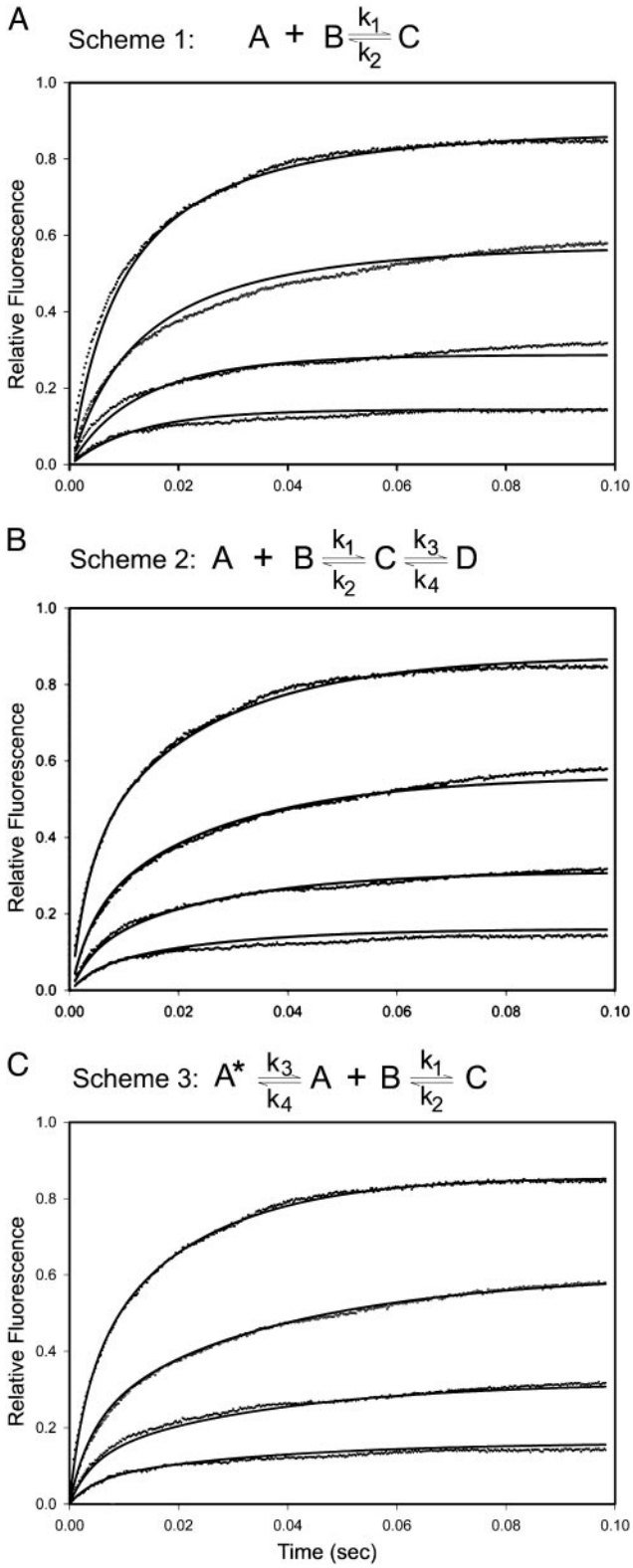

Fig. 2. Kinetic analysis of tau* binding to taxol-stabilized microtubules. Taxol-stabilized microtubules (2.3 μM after mixing) and tau* (1.4, 0.70, 0.35, and 0.175 μM after mixing, top to bottom) in BRB-80 buffer/5 μM taxol/0.125 mM GTP were mixed rapidly in a stopped-flow fluorometer, and the time-dependent change in fluorescence caused by FRET was recorded. The best-fit curves (—) are superimposed on the raw data. Each curve represents the average of three to five individual traces. *A–C* show the best-fit curves to the data when reaction schemes 1–3, respectively, were used for fitting. An independent replicate experiment gave similar results (data not shown).

Table 1. Kinetic parameters for the binding of tau* to taxol-stabilized microtubules

Parameter†	Optimized value‡
k_1	294 ± 18 $\mu M^{-1}\cdot s^{-1}$
k_2	2.5 ± 0.9 s^{-1}
k_3	35 ± 3 s^{-1}
k_4	31 ± 4 s^{-1}
N§	0.29 ± 0.003
K_D¶	16 ± 5 nM

†Refer to scheme 3 of Fig. 2*C*.
‡Values are the mean of two independent experiments; errors are propagated from standard deviation values (n = number of data points) derived from each experiment.
§Maximal stoichiometry of tau:tubulin dimer.
¶Calculated: $K_D = (k_2/k_1)(1 + k_4/k_3)$.

nM]. Thus, we conclude from both kinetic fitting and independent thermodynamic measurements that scheme 3 provides the best fit to the data and suggest that a conformational change in tau*, microtubules, or both occurs before interaction.

Kinetic Simulation Studies. A key observation from the kinetic studies is the fast dissociation rate of tau from preassembled microtubules (k_2 = 2.5 s^{-1}; $t_{1/2}$ = 280 ms). Although the rate-constant values in Table 1 provide the best fit to the data, we tested for the possibility of other solutions to the binding mechanism. To do this, we carried out kinetic simulations to determine whether the experimental data could be consistent with the slow release of tau*. When the overall K_D value was constrained to the experimentally determined value of 14 nM (Fig. 3), we found that a dissociation rate constant (k_2) of 1 s^{-1} could not accommodate the data (data not shown). Even when the K_D value was constrained to 2 nM, the corresponding rate of dissociation was 0.16 s^{-1} ($t_{1/2}$ = 4.3 s). Under these conditions, complete exchange with the bulk solvent would be expected after ≈25 s (6 × $t_{1/2}$). Thus, given the known thermodynamics of tau binding to taxol-stabilized microtubules, we conclude that dissociation must necessarily be fast.

Equilibrium Competition Between Labeled and Unlabeled Tau. Given the fast association rate between tau and taxol-stabilized microtubules (k_1 = 294 $\mu M^{-1}\cdot s^{-1}$), the fast rate of dissociation (k_2 =

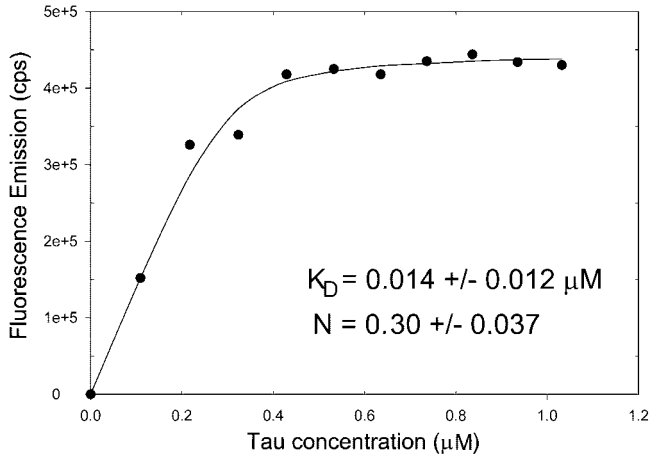

Fig. 3. Equilibrium binding of tau* to taxol-stabilized microtubules. Tau* was added to microtubules (1 μM tubulin in BRB-80/5 μM taxol/0.125 mM GTP) or buffer. Binding was monitored by energy transfer, and data were analyzed as described in *Experimental Procedures*.

$2.5\ s^{-1}$) is inconsistent with a stable interaction between tau and microtubules, as demonstrated originally by radioisotope-exchange studies (3, 12). Thus, we sought to determine whether this discrepancy could be attributed to the manner in which the tau–microtubule complex was formed.

Fig. 4 shows the fluorescence emission caused by FRET in equilibrium-competition experiments. In these experiments, tau* is either bound to preassembled microtubules (stabilized with or without taxol) or incorporated into microtubules during microtubule assembly and then subsequently chased with excess unlabeled tau. In all cases, competition was found to be complete within the dead time of manual mixing (<20 s), which is consistent with a fast dissociation rate of tau ($t_{1/2} < 3$ s), as demonstrated by stopped-flow analysis (Table 1). The fluorescence emission traces subsequent to competition were stable over an extended time period (up to 30 min), suggesting that in all cases equilibrium had been reached.

Extent of Competition. ***Taxol-stabilized microtubules.*** The amplitude of the fluorescence change in response to competition shows the extent to which tau* was chased effectively from microtubules by unlabeled tau. Competition of tau* from taxol-stabilized microtubules resulted in a decrease in fluorescence emission to a level exactly matching that of an equilibrium mixture of an equivalent concentration ratio of tau*, unlabeled tau, and microtubules (Fig. 4*A*). Thus, the binding of tau* to taxol-stabilized microtubules seems to be governed by a classical equilibrium that is rapid and completely reversible.

Taxol-free microtubules. It has been hypothesized that taxol may compete directly with tau for the binding of microtubules (13). Thus, it is possible that the more weakly bound tau on the surface of taxol-stabilized microtubules was an artifact attributable to the presence of taxol as opposed to being an intrinsic property of the tau–microtubule interaction *per se*. To determine the possible effect of taxol on tau binding, we carried out competition experiments using taxol-free preassembled microtubules (Fig. 4*B*). The fluorescence emission of tau* bound to these microtubules was similar to that with taxol-stabilized microtubules (Fig. 4*A*) and, after addition of unlabeled tau, the fluorescence was similarly reduced to baseline levels. Thus, tau* binds to taxol-stabilized, as well as to taxol-free, microtubules to generate a single population of microtubule-bound tau* that undergoes rapid and complete exchange with free tau.

Microtubules polymerized in the presence of tau. Either taxol or MAPs such as tau act to significantly lower the critical concentration for microtubule polymer formation from free tubulin. To test the kinetic behavior of tau incorporated into microtubules during the assembly process, we assembled microtubules in the presence of tau*. Similar to that of tau* bound to preassembled microtubules, a portion of the fluorescence signal could be chased rapidly after the addition of excess unlabeled tau. In contrast, however, a significant proportion (≈50%) of the specific signal caused by FRET remained (Fig. 4*C*) even after prolonged incubation. Thus, these experiments reveal two separate populations of microtubule-bound tau* that can be distinguished in competition experiments: one that is easily chased from microtubules displaying a half-life in the millisecond time scale and a second that seems irreversibly bound. A lower limit for the half-time of the latter is on the order of at least several hours. The existence of two distinct populations of microtubule-bound tau* is consistent with an ≈20-nm Stokes shift observed in the fluorescence emission maximum wavelength associated with tau* bound to preassembled microtubules (λ_{max} = 493 nm) versus tau* incorporated into microtubules during microtubule assembly (λ_{max} = 476 nm), suggesting distinct environments that surround the acrylodan molecule (Fig. 5).

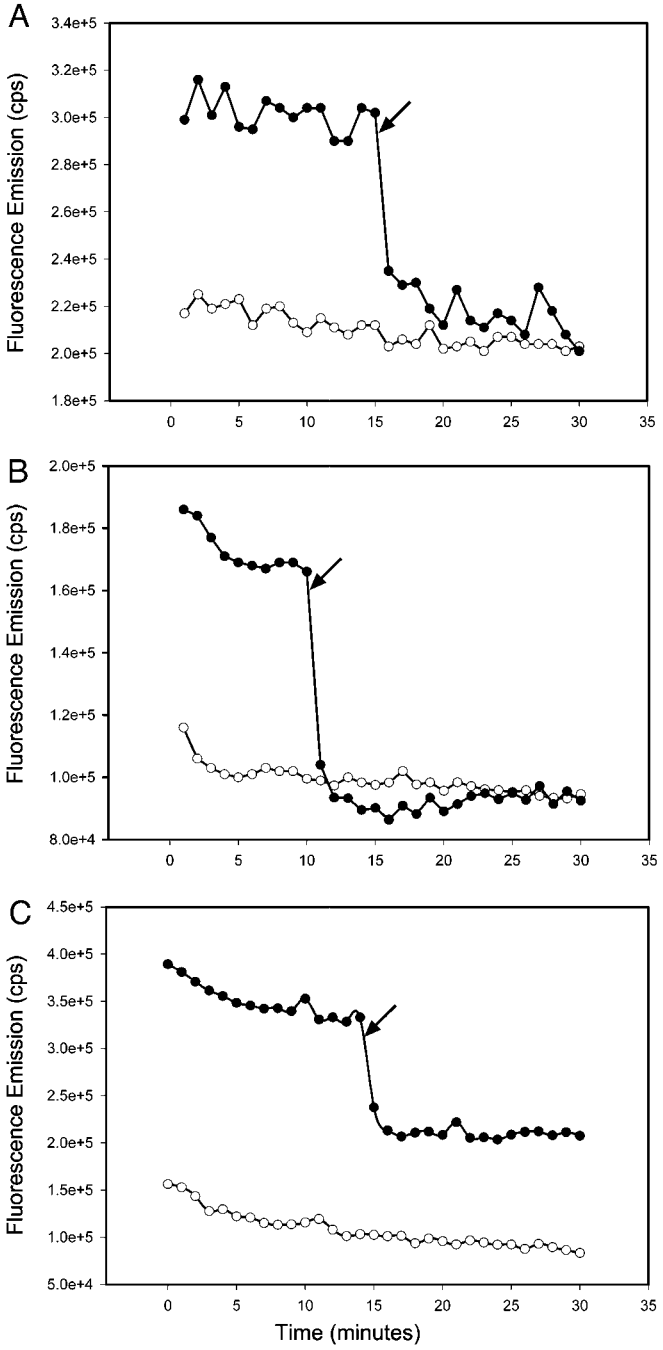

Fig. 4. Competition between tau* and unlabeled tau. Shown is fluorescence emission caused by energy transfer (λ_{ex} = 280 nm, λ_{em} = 497 nm) arising from tau* bound to taxol-stabilized microtubules (*A*), bound to taxol-free microtubules (*B*), and coassembled with free tubulin to form a tau–microtubule copolymer (*C*). Tau* = 0.25 μM; microtubules = 1.25 μM tubulin; GTP = 0.125 mM; taxol (*A*) = 20 μM. Arrows indicate the addition of 2.5 μM unlabeled tau (●). Baseline fluorescence corresponds to the addition of an equivalent equilibrium mixture of tau*/unlabeled tau (1:10) to preassembled microtubules or free tubulin (○). Results are typical of three independent experiments performed.

Discussion

Studies on the mechanism of interaction between tau and microtubules invoke a paradox that, to date, has not been addressed. Early work suggests that tau dissociates from microtubules with extremely slow kinetics, evident by the lack of

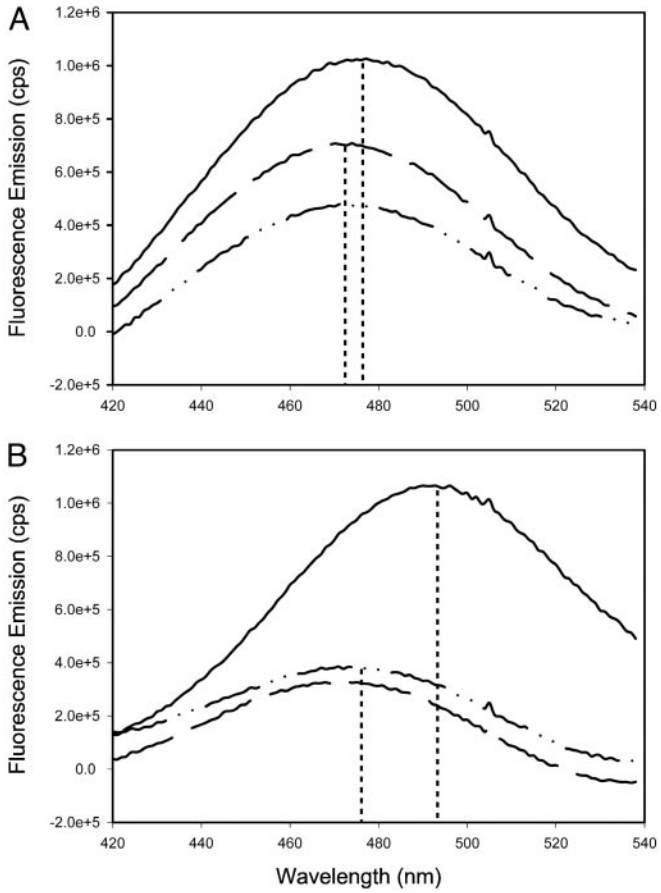

Fig. 5. Emission spectra of tau* copolymerized with microtubules or bound to taxol-stabilized microtubules. (*A*) Tau* copolymerized with microtubules. (*B*) Tau* bound to preassembled taxol-stabilized microtubules. Microtubule-associated tau* (—), microtubule-associated tau* after chase with 10-fold excess unlabeled tau (– – –), and baseline as described in the Fig. 4 legend (- - -). Microtubules = 1.25 μM tubulin; tau* = 0.25 μM; taxol = 20 μM; the buffer was BRB-80/0.125 mM GTP; λ_{ex} = 280 nm.

exchange of two different populations of radiolabeled microtubule-bound tau (3, 12). Here we have analyzed the tau–microtubule interaction in kinetic detail using an acrylodan-labeled derivative of tau. The kinetic mechanism describing the binding of tau* to preassembled-microtubules involves fast dissociation of tau from taxol-stabilized microtubules, which is inconsistent with tight, nonexchangeable binding. Equilibrium-competition experiments provide an explanation for this paradox by demonstrating that two distinct populations of microtubule-bound tau can exist: one that corresponds to the reversible binding of tau, most likely to the surface of preassembled microtubules (independent of taxol-stabilization), and a second that corresponds to the irreversible incorporation of tau into microtubules during net polymer formation.

Kinetic Pathway for Binding. Kinetic analysis by stopped-flow rapid-mixing techniques reveals that the overall binding reaction between tau and preassembled microtubules is a multistep process. In all the kinetic studies, low concentrations of tau were used, because at high concentrations anomalous kinetic traces were seen that were uninterpretable. This observation is consistent with the work of Ackmann *et al*. (10), who showed classic hyperbolic binding of tau to microtubules at low tau concentrations followed by linear, nonsaturable binding at higher tau concentrations.

The minimal kinetic scheme for overall binding is comprised of two steps that include a "conformational change" (for lack of evidence of any other type of chemistry) that necessarily occurs before bimolecular encounter (Fig. 2*C*, scheme 3). The model given by scheme 3 (Fig. 2*C*) and Table 1 is supported by the following observations: (*i*) both the K_D value and the maximal stoichiometry of binding derived from kinetic analysis or measured by thermodynamic titration are the same and in turn are consistent with literature values; (*ii*) the fast off-rate (k_2) inferred from stopped-flow analysis is consistent with equilibrium-competition experiments [competition is complete within the dead time of manual mixing (<20 s)]; (*iii*) regression analyses consistently converged on the same least-squares minimum starting from widely ranging initial parameter values (data not shown); and (*iv*) a search for possible alternate solutions to the kinetic mechanism by computer simulation was unsuccessful when fitting was constrained by an independently measured K_D value.

The reaction pathway proposed is consistent with conformational changes in tau, microtubules, or both. Furthermore, we cannot speculate on the nature or magnitude of such changes in conformation. Tau is known to be largely unstructured (14, 15) and flexible in solution, and its flexibility is reduced after binding microtubules (16). Thus, relevant changes in conformation may correspond to the net interconversion of various conformers of tau, only one of which binds microtubules. In addition, the kinetic data do not exclude a more complex mechanism that may be comprised of additional conformational changes in either unbound microtubules and/or the tau–microtubule complex. For example, we have reported previously that, subsequent to microtubule binding, tau may undergo oligomerization to form tau dimers or higher-order tau oligomers on the microtubule surface (17). In addition, a small (8-aa) tau peptide seems to be capable of altering microtubule dynamics at a distance (11), and atomic force microscopy studies show apparent reorganization of the microtubule surface after tau binding (17). These data infer conformational changes in the tau–microtubule complex subsequent to bimolecular encounter. Therefore, it is reasonable to expect that the complete mechanism by which free tau binds to the microtubule surface is comprised of a complex multistep pathway, of which we have been able to kinetically isolate two steps (scheme 3, Fig. 2*C*).

Two Distinct Sites for Tau on Microtubules. The stable interaction historically observed between tau and microtubules is found when free tubulin is assembled in the presence of tau. Under these conditions, tau and tubulin are copolymerized during net microtubule polymer formation. By comparison, ligand-binding studies examining the interaction between tau and microtubules traditionally have used microtubules that were preassembled and stabilized with taxol. We therefore examined the kinetic properties of the tau*–microtubule complex formed under either of these conditions. When microtubules were assembled in the presence of tau*, competition with unlabeled tau revealed two distinct populations of bound tau: one that was exchangeable and a second that was not. In contrast, we found that all of the tau* bound to preassembled, taxol-stabilized microtubules was exchangeable. The weaker binding at the exchangeable site is not caused by competition from taxol, because the same results were obtained by using taxol-free microtubules. Thus, the kinetic behavior and affinity of tau bound to microtubules seems to depend on the conditions under which tau is incorporated into the tau–microtubule complex. We speculate that during net microtubule assembly, tau may become irreversibly incorporated into the fabric of the microtubule wall, whereas tau bound to the surface of preassembled microtubules remains readily exchangeable with the medium.

In support of our observations, three studies addressing the

structure of microtubule-bound tau have reported results that correlate with the manner in which the bound complex was prepared. Cryoelectron microscopy analysis of MAP2- or tau-saturated microtubules (18) shows evidence for solely longitudinal binding of tau on microtubule protofilament ridges. On the other hand, analysis by atomic force microscopy of low levels of microtubule-bound tau detected the possible formation of tau oligomers that encircle microtubules, perhaps functioning to strengthen lateral interactions and/or produce a concerted (and stabilizing) allosteric shift in microtubule conformation (17). In each of these cases, preassembled taxol-stabilized microtubules were used. In contrast, cryoelectron microscopy performed on microtubules assembled with tau in the absence of taxol revealed detectable tau in the microtubule lumen (13). In this study, it was proposed that taxol and tau compete for the same internal microtubule-binding site. The results presented herein do not address this hypothesis. For example, although taxol does not compete with peripherally bound tau, we cannot rule out the possibility that the nonexchangeable binding site for tau and taxol may be the same.

Furthermore, our data do not address the physical basis for two kinetically distinct sites. We imagine that such sites may be physically distinct or, alternatively, may overlap significantly. For example, although it is commonly accepted that tau interacts with the C terminus of tubulin (18, 19), earlier work by Littauer *et al*. (20) demonstrated that the N terminus of α-tubulin also may bind tau. Thus, reversible binding may correspond to conditions in which tau binds to one or the other of these regions, whereas irreversible binding may result under conditions in which tau binds to the alternate or both regions of tubulin.

Tau is a MAP that is highly enriched in neurons and is essential for the regulation of microtubule function. The majority of *in vitro* studies have used preassembled microtubules to characterize the binding of tau. For example, the effects of tau phosphorylation associated with Alzheimer's disease and those of mutations in tau associated with frontotemporal dementia with parkinsonism linked to chromosome 17 (21) have been correlated with defects in the binding of tau to preassembled microtubules (9, 22). *In vivo*, however, tau is expected to be copolymerized with tubulin during the normal process of microtubule assembly/disassembly. We have shown that tau in such a copolymer displays dramatically different interaction properties with microtubules. We suggest that tau in the coassembled polymer may be relevant to the mechanism by which disease-related modifications of tau may result in tau dysfunction and neuropathology.

We thank Dr. Mary Ann Jordan for advice and critical reading of the manuscript; Dr. Kevin Plaxco, Miguel DelosRios, and Dr. Blake Gillespie for providing stopped-flow instrumentation; and Dr. Les Wilson and Herb Miller for supplying purified tubulin. This work was supported by National Institutes of Health Grant GM58445 and California Alzheimer's Society Grant 23-15941.

1. Jordan, M. A. (2002) *Curr. Med. Chem. Anti-Cancer Agents* **2,** 1–17.
2. Lee, V. M., Goedert, M. & Trojanowski, J. Q. (2001) *Annu. Rev. Neurosci.* **24,** 1121–1159.
3. Weingarten, M. D., Lockwood, A. H., Hwo, S. Y. & Kirschner, M. W. (1975) *Proc. Natl. Acad. Sci. USA* **72,** 1858–1862.
4. Butner, K. A. & Kirschner, M. W. (1991) *J. Cell Biol.* **115,** 717–730.
5. Gustke, N., Trinczek, B., Biernat, J., Mandelkow, E. M. & Mandelkow, E. (1994) *Biochemistry* **33,** 9511–9522.
6. Goode, B. L. & Feinstein, S. C. (1994) *J. Cell Biol.* **124,** 769–782.
7. Goode, B. L., Denis, P. E., Panda, D., Radeke, M. J., Miller, H. P., Wilson, L. & Feinstein, S. C. (1997) *Mol. Biol. Cell* **8,** 353–365.
8. Goode, B. L., Chau, M., Denis, P. E. & Feinstein, S. C. (2000) *J. Biol. Chem.* **275,** 38182–38189.
9. Hong, M., Zhukareva, V., Vogelsberg-Ragaglia, V., Wszolek, Z., Reed, L., Miller, B. I., Geschwind, D. H., Bird, T. D., McKeel, D., Goate, A., *et al*. (1998) *Science* **282,** 1914–1917.
10. Ackmann, M., Wiech, H. & Mandelkow, E. (2000) *J. Biol. Chem.* **275,** 30335–30343.
11. Panda, D., Daijo, J. E., Jordan, M. A. & Wilson, L. (1995) *Biochemistry* **34,** 9921–9929.
12. Job, D., Pabion, M. & Margolis, R. L. (1985) *J. Cell Biol.* **101,** 1680–1689.
13. Kar, S., Fan, J., Smith, M. J., Goedert, M. & Amos, L. A. (2003) *EMBO J.* **22,** 70–77.
14. Cleveland, D. W., Hwo, S. Y. & Kirschner, M. W. (1977) *J. Mol. Biol.* **116,** 227–247.
15. Schweers, O., Schonbrunn-Hanebeck, E., Marx, A. & Mandelkow, E. (1994) *J. Biol. Chem.* **269,** 24290–24297.
16. Woody, R. W., Clark, D. C., Roberts, G. C., Martin, S. R. & Bayley, P. M. (1983) *Biochemistry* **22,** 2186–2192.
17. Makrides, V., Shen, T. E., Bhatia, R., Smith, B. L., Thimm, J., Lal, R. & Feinstein, S. C. (2003) *J. Biol. Chem.* **278,** 33298–33304.
18. Al-Bassam, J., Ozer, R. S., Safer, D., Halpain, S. & Milligan, R. A. (2002) *J. Cell Biol.* **157,** 1187–1196.
19. Chau, M. F., Radeke, M. J., de Ines, C., Barasoain, I., Kohlstaedt, L. A. & Feinstein, S. C. (1998) *Biochemistry* **37,** 17692–17703.
20. Littauer, U. Z., Giveon, D., Thierauf, M., Ginzburg, I. & Ponstingl, H. (1986) *Proc. Natl. Acad. Sci. USA* **83,** 7162–7166.
21. Hasegawa, M., Smith, M. J. & Goedert, M. (1998) *FEBS Lett.* **437,** 207–210.
22. Barghorn, S., Zheng-Fischhofer, Q., Ackmann, M., Biernat, J., von Bergen, M., Mandelkow, E. M. & Mandelkow, E. (2000) *Biochemistry* **39,** 11714–11721.